Selected Paper

Structures and Magnetic Properties of First-Row Transition Metal Complexes with Bridging Ligands, Squarate or Pyrazine

Akiko Jimbo-Kobayashi, Akiko Kobayashi,* Itaru Tamura,[1,†] Nao Kawada,[2] and Takeshi Miyamoto[2]

Research Centre for Spectrochemistry, Graduate School of Science, The University of Tokyo, Hongo, Bunkyo-ku, Tokyo 113-0033

[1]Institute for Molecular Science, Okazaki, Aichi 444-8585

[2]Department of Chemistry, School of Science, Kitasato University, Sagamihara, Kanagawa 228-8555

Received September 15, 2004; E-mail: akiko@chem.s.u-tokyo.ac.jp

For the purpose of construction of the hydrogen-bonded and coordination-bonded supramolecular network, Mn^{II} complex bridged by squarate molecules was synthesized, and their structural and magnetic properties were studied. X-ray structure determination revealed that Mn^{II} complex, $[Mn^{II}_4(C_4O_4)_4(C_4H_4N_2)(H_2O)_8]$, had a three-dimensional network structure bridged by squarates with cavities which trap pyrazine molecules. Pyrazine molecules have an orientational disorder even at 10 K in the cavities. They are stabilized by weak hydrogen bonds with a network formed by squarates. A weak antiferromagnetic exchange interaction is observed between magnetic moments on Mn^{2+} ions through squarate. In the case of one-dimensional polymer chain complexes, $M^{II}(C_4O_4)(C_4H_4N_2)(H_2O)_4$ (where $M^{II} = Fe^{II}$, Ni^{II}, Cu^{II}), which are bridged by pyrazine molecules, the temperature dependence of magnetic susceptibility follows Bonner–Fischer's one dimensional chain model. The antiferromagnetic exchange parameter for Cu^{II} complex is slightly larger than those for Fe^{II} and Ni^{II} complexes. This difference is considered to be caused by the difference of the metal to metal distances. In the case of $[Co^{II}(C_4O_4)(C_4H_4N_2)(H_2O)_4]$, clear anisotropy of the magnetic properties was observed, which was caused by large zero-field splitting.

Recently the concept of supramolecule attracted interest from the structural aspect and from its potential technological applications.[1,2] Especially molecular networks which have cavities and channels receive considerable attention as materials which have host–guest interactions.[3–6] For construction of supramolecular metal–organic open frameworks, the use of polytypic organic linkers has become an attractive strategy. Furthermore, the construction of metal–organic complex with molecular network structure opens the possibility of designing functional supramolecule with additional physical properties. Under these concepts, we focused on 3,4-dihydroxy-3-cyclobutene-1,2-dione (squaric acid, $H_2C_4O_4$) and 1,4-diazine (pyrazine) as multiconnecting ligands for metal–organic frameworks.

Squaric acid was synthesized by Cohen et al. in 1959.[7] Squarate dianion was reported to be stabilized by delocalization of electrons.[8] Squarate dianion acts as a bridging ligand for transition metals to form transition metal squarate complex dimer or polymer.[9,10] As squaratomanganese(II) complexes, $Mn^{II}(C_4O_4)(H_2O)_2$ and $Mn^{II}(HC_4O_4)_2(H_2O)_4$ are known.[11] In case of $Mn^{II}(C_4O_4)(H_2O)_2$, it was shown that acetic acid hydrate molecules or water molecules were incorporated in its voids to form clathrate polymer *catena*-[tetraaqua(μ_4-squarato)diaquamanganese(II)]acetic acid hydrate][12] or poly[[diaqua(μ_4-squarato-*O*,*O*′,*O*″,*O*‴)-manganese(II)]0.93-hydrate].[13] Acetic acid hydrate was suggested to reside in the voids, which was only detected by the elemental analysis. The water molecule was detected by the single crystal structure determination, but its behavior as a guest molecule was not evident.

The collective properties shown in supramolecules on magnetism are also of interest from both theoretical and experimental aspects.[14] Enough data on magneto-structural correlation are expected to enable us to design new materials with new magnetic properties. A pyrazine molecule is known to form a bridged low-dimensional polymer complex when it coordinates to transition metals.[15] Recently pyrazil complexes of first-row transition metals $[M^{II}(C_4O_4)(C_4H_4N_2)(H_2O)_4]$ ($M = Fe^{II}$, Co^{II}, Ni^{II}, Cu^{II}) with squarate dianion which formed intermolecular hydrogen bonds were synthesized and their one-dimensional structures were reported.[16,17]

In this study, we present the single crystal structure of squaratomanganese(II) complex which trapped pyrazine molecules in its cavities by the low temperature X-ray structural determination. And we also present temperature dependences of magnetic susceptibilities of one-dimensional chain complexes bridged by pyrazine molecules ($[M^{II}(C_4O_4)(C_4H_4N_2)(H_2O)_4]$ ($M^{II} = Fe^{II}$, Co^{II}, Ni^{II}, Cu^{II}). Considering their one-dimensional polymer structure, the difference of magnetic interactions between magnetic moments on metal cations will be of great interest. We will discuss the correlation between their crystal structures and their magnetic properties.

Experimental

General Information. All starting materials were purchased from commercial sources. Elemental analyses of products were

† Present address: Japan Atomic Energy Research Institute, Tokai-mura, Ibaraki 319-1195

Published on the web March 11, 2005; DOI 10.1246/bcsj.78.445

performed on crystalline samples by Elemental Analysis Laboratory at the Department of Chemistry, University of Tokyo. Infrared spectra were measured from KBr pellets using a JEOL FT-IR-420 system.

Preparation of Compounds. $[Mn^{II}_4(C_4O_4)_4(C_4H_4N_2)(H_2O)_8]$ (1): Equal volumes (2.5 mL) of aqueous solutions of 0.144 M manganese(II) chloride tetrahydrate ($MnCl_2 \cdot 4H_2O$) and 0.288 M of pyrazine (1,4-$C_4H_4N_2$) were mixed to give a pale pink clear solution. To this mixture, 7.5 mL of 0.045 M aqueous squaric acid ($H_2C_4O_4$) solution was added. The mixed solution was kept for a few days and pale pink polyhedral crystals were deposited at room temperature. They were collected and washed with water, followed by ethanol, and were air dried to give 10.4 mg (13.0%) of product. The product was insoluble in water and common organic solvents. Anal. Found: C, 26.83; H, 2.18; N, 3.22%. Calcd for $C_{20}H_{20}N_2O_{24}Mn_4$: C, 26.93; H, 2.26; N, 3.14%. Characteristic IR absorptions (KBr pellet, 400–4000 cm^{-1}) 3277s (ν_{OH}), 2224m (ν_{CC}), 1511s (ν_{CO+CC}), 1155w (δ_{CH}), 1099s (ν_{CC}), 1018w (δ_{CH}), 810w (δ_{CH}). Density: Calcd. 1.953. Obsd. 1.959.

$[Zn^{II}(C_4O_4)(C_4H_4N_2)(H_2O)_4]$ (6): This complex was prepared by a method similar to that used for Mn^{II} complex (**1**). Yellow plate crystal. Yield: 35%. Anal. Found: C, 28.98; H, 3.62; N, 8.48%. Calcd for $C_8H_{12}N_2O_8Zn$: C, 29.15; H, 3.67; N, 8.50%. Characteristic IR absorptions 3215s (ν_{OH}), 2208m (ν_{CC}), 1483s (ν_{CO+CC}), 1152w (δ_{CH}), 1091s (ν_{CC}), 1057w, 1001w (δ_{CH}), 817w (δ_{CH}).

$[M^{II}(C_4O_4)(C_4H_4N_2)(H_2O)_4]$ ($M = Fe^{II}$ (2), Co^{II} (3), Ni^{II} (4), Cu^{II} (5)): These complexes were prepared at room temperature for magnetic measurements by a method similar to that used for Mn^{II} complex (**1**). In case of Cu^{II} complex (**5**), single crystals have been obtained so far only by use of silica gel medium for crystal growth.[17] Fe^{II} (**2**), Co^{II} (**3**) and Ni^{II} (**4**) complexes have been synthesized under hydrothermal conditions at 150 °C.[16] This time, by controlling the solution concentration, single crystals of Fe^{II}, Ni^{II}, Co^{II}, Cu^{II}, and Zn^{II} complexes with pyrazine and squarate large enough for single crystal X-ray structure determination were obtained from aqueous solution at room temperature. They were identified by the elemental analyses, IR mesurements and single crystal X-ray structure determinations.

X-ray Crystallographic Mesurements. Single crystals of Mn^{II} complex (**1**) suitable for X-ray structure determination with dimensions of $0.20 \times 0.20 \times 0.20$ mm were chosen and the crystal structure determination at 10 K was performed by a Weissenberg-type imaging plate system (Mac Science DIP-320) with a helium refrigerator. Temperature dependences of cell parameters and of the cell volumes of manganese complexes were also measured from room temperature down to 10 K. Crystal structural data for compounds of Zn^{II} complex (**6**) were collected at room temperature on a RIGAKU Mercury CCD X-ray system. The experimental details on Mn^{II} complex (**1**) and Zn^{II} complex (**6**) are summarized in Table 1. The structures were solved by direct methods and refined by full-matrix least squares. Selected bond lengths and angles are given in Tables 2 and 3. About Fe^{II} complex (**2**), Co^{II} complex (**3**), Ni^{II} complex (**4**), and Cu^{II} complex (**5**), we used the reported crystal data.[16,17]

Magnetic Measurements. Magnetic susceptibility measurements of polycrystal samples of Mn^{II} complex (**1**), Fe^{II} complex (**2**), Ni^{II} complex (**4**), and Cu^{II} complex (**5**) were performed over the temperature range from 2 K to 300 K in an applied magnetic field of 0.5 T with a Quantum Design SQUID magnetometer. Diamagnetic susceptibility was estimated from Pascal's constants. In the case of Co^{II} complex (**3**), magnetic susceptibilities of the single crystal sample were measured over the same temperature range in applied magnetic field of 1 T. The angular dependent measurements of Co^{II} complex (**3**) were performed by applying the magnetic field parallel to the *a*-axis, the *b*-axis and the *c*-axis of the single crystal, respectively. For a single crystal of Cu^{II} complex (**5**), the same angular dependent measurements as Co^{II} complex (**3**) were performed under the magnetic field of 0.5 T.

Table 1. Crystallographic Data of $[Mn^{II}_4(C_4O_4)_4(C_4H_4N_2)(H_2O)_8]$ (**1**) and $[Zn^{II}(C_4O_4)(C_4H_4N_2)(H_2O)_4]$ (**6**)

	1	**6**
Formula	$C_{20}H_{20}N_2O_{24}Mn_4$	$C_8H_{12}N_2O_8Zn$
a/Å	16.544(6)	7.181(10)
b/Å	16.544(6)	11.31(2)
c/Å	16.544(6)	7.253(10)
α/deg		
β/deg		91.11(2)
γ/deg		
V/Å^3	4534(1)	587.5(12)
Z	6	2
Formula weight	891.13	329.58
Crystal system	Cubic	Monoclinic
Space group	$Pn\bar{3}n$	$P2_1/n$
T/K	10	300
ρ(obsd)/g cm^{-3}	1.959	
ρ(calcd)/g cm^{-3}	1.953	1.86
μ/cm^{-1}	17.32	17.32
R[a)]	0.044	0.045
R_w[b)]	0.052	0.062
λ/Å	0.71069	0.71069

a) $R = \Sigma(|F_0| - |F_c|)/\Sigma|F_0|$. b) $R_w = [\Sigma w(|F_0| - |F_c|)^2]/\Sigma w F_0{}^2]^{1/2}$.

Table 2. Selected Bond Lengths (Å) and Angles (deg) for $[Mn^{II}_4(C_4O_4)_4(C_4H_4N_2)(H_2O)_8]$ (**1**)

Mn–O(1)	2.172(6)	O(1)–Mn(1)–O(3)	88.4(2)
Mn–O(3)	2.189(6)	O(1)–Mn(1)–O(2)	96.3(2)
O(3)–C(2)	1.255(9)	O(2)–Mn(1)–O(3)	93.6(2)
C(2)–C(2)	1.48(1)	O(1)–Mn(1)–O(1)	89.2(2)
Mn(1)–O(2)	2.136(5)	O(3)–Mn(1)–O(3)	94.0(2)
O(1)–C(1)	1.266(9)		
C(1)–C(1)	1.45(1)		

Table 3. Selected Bond Lengths (Å) and Angles (deg) for $[Zn^{II}(C_4O_4)(C_4H_4N_2)(H_2O)_4]$ (**6**)

Zn(1)–O(1)	2.083(6)	O(1)–Zn(1)–O(2)	89.8(3)
Zn(1)–O(2)	2.088(6)	O(1)–Zn(1)–N(1)	88.8(3)
Zn(1)–N(1)	2.202(5)	O(2)–Zn(1)–N(1)	89.6(3)
N(1)–C(3)	1.315(9)	Zn(1)–N(1)–C(3)	121.3(5)
N(1)–C(4)	1.345(9)	Zn(1)–N(1)–C(4)	122.1(5)
C(1)–C(2)	1.445(10)	O(3)–C(1)–C(2)	134.6(7)
C(2)–C(1)	1.436(10)	O(4)–C(2)–C(1)	135.1(7)
C(3)–C(4)	1.381(9)		
C(2)–O(4)	1.267(8)		
C(1)–O(3)	1.289(8)		
C(3)–H(1)	0.85(7)		
C(4)–H(2)	0.93(7)		

Results and Discussion

$[Mn^{II}_4(C_4O_4)_4(C_4H_4N_2)(H_2O)_8]$ (1). The crystal structure of Mn^{II} complex (**1**) at 10 K was examined. Mn^{2+} cations are coordinated by four squarates and two water molecules in a distorted octahedral fashion. Four oxygen atoms in one squarate anion coordinate to four different Mn^{2+} cations (Fig. 1(a)) to construct a three-dimensional network. The broad and symmetrical absorption band near 1500 cm^{-1} in the infrared spectrum indicates that squarate has D_{4h} symmetrical structure by coordinating to four different Mn^{2+} cations with four oxygen atoms in a similar fashion.

Temperature dependence of cell parameters and cell volumes were measured from room temperature down to 10 K. The change of cell volume was 0.5% even at 10 K. This small value reveals that the 3-D network structure is rigid and that no structural change occurs within this temperature range. This rigidity is considered to be caused by a hydrogen-bonded web. The 3-D network consisting of manganese cations and squaric anions is also connected by hydrogen bonds between water molecules and squarate dianions (Fig. 1(b)). One oxygen atom on squarate anion coordinates to one Mn^{2+} cation. This squarate oxygen atom is also hydrogen-bonded to a water molecule coordinated to another Mn^{2+} cation. If only C, O, and Mn atoms are considered, there is a hexagonal ring formed by Mn, half of squarate anion and one water molecule, shown as Mn1–O3–C2–C2*–O3*–O2 in Fig. 1(b). This web is considered to stabilize 3-D network structure and keep it rigid.

X-ray single crystal determination revealed that the pyrazine molecules occupied cavities formed by the Mn–squarate three-dimensional network. The pyrazine molecule has an orientational disorder even at 10 K in the cavity. There are two kinds of pyrazine molecules, whose orientations are different by 90° around the N–N axis (Fig. 2).

Steiner and Desiraju suggested that C–H groups could act as weak hydrogen bond donors and that the H···O distance cutoff could be selected to be $d = 3.0$ Å.[18] The distances of C–H on pyrazine molecules were evaluated to be from 0.85 Å to 0.93 Å for $[Zn^{II}(C_4O_4)(C_4H_4N_2)(H_2O)_4]$ complex by X-ray crystal structure determination (Table 3). The X-ray single crystal structure determination of pyrazine molecule suggested that the C–H bond length was from 0.92 Å to 0.94 Å.[19] Using these values, we can estimate a distance less than $D = 3.85$ Å (D is the distance between C and O through hydrogen atom.) to be possible for the weak hydrogen bonds. Three weak hydrogen bonds between each carbon atom of pyrazine molecule (C(3)) and oxygens on squarates (O(3)) which have the distances less than 3.85 Å were found at 10 K, as shown in Fig. 2. This fact suggests that weak hydrogen bond interactions C–H···O stabilize pyrazine molecules in the cavities. This possibility is supported by another report which suggests the existence of C–H···N interaction within pyrazine crystals.[20]

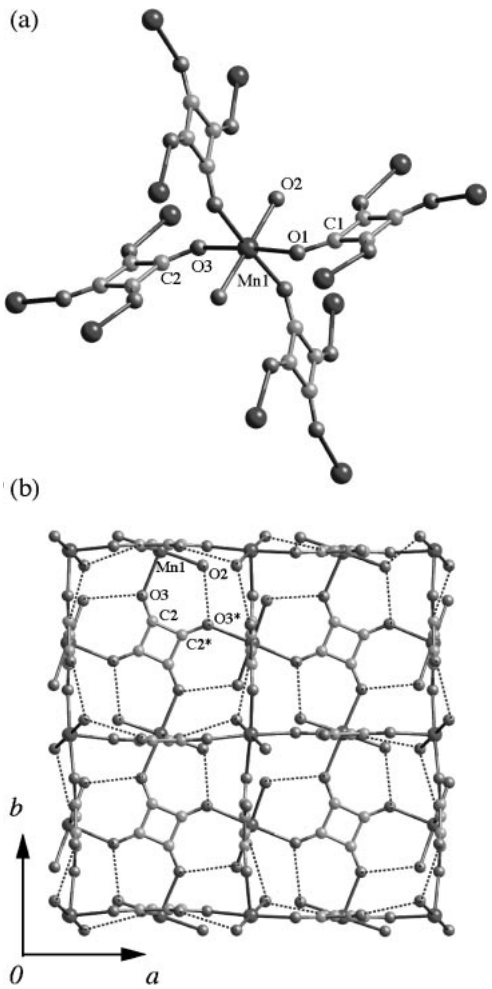

Fig. 1. (a) Local coordination environment for $[Mn^{II}_4(C_4O_4)_4(C_4H_4N_2)(H_2O)_8]$ showing the atom labeling scheme. Hydrogen atoms are omitted for clarity. (b) Three-dimensional network structure of Mn(II) complex (**1**) viewed from the [001] direction. Dashed lines represent hydrogen bonds between water molecules and squarate dianions. A hexagonal ring Mn1–O3–C2–C2*–O3*–O2 formed by Mn, half of squarate anion, and one water molecules is shown. Pyrazine molecules are omitted.

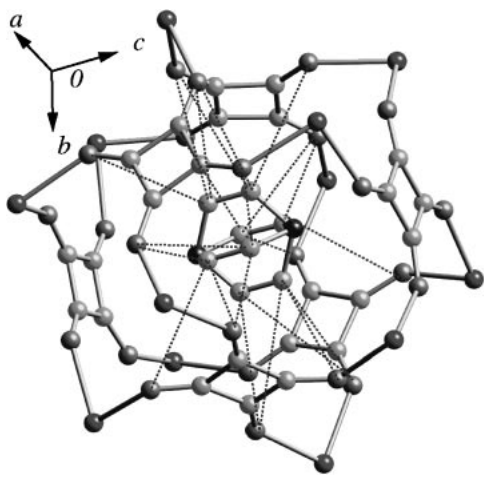

Fig. 2. Pyrazine molecule stabilized in the cavity by weak hydrogen bonds between pyrazine molecule and squarate for $[Mn^{II}_4(C_4O_4)_4(C_4H_4N_2)(H_2O)_8]$ complex (**1**). Orientationally different two pyrazine molecules exit in the cavity. Dashed lines express weak hydrogen bonds between C–H of pyrazine molecule and O atoms on squarates.

Several studies indicated that acetic acid hydrate or water molecules were incorporated into the voids of squaratomanganese(II) complex as guest molecules.[12,13] However, no information on interaction between guest molecules and the host molecule was obtained so far. This time we could verify the orientations of small pyrazine molecules trapped in the cavity of Mn^{II} complex by low temperature X-ray single crystal structure determination. And we also indicated that they were fixed in the cages by weak hydrogen bonds and did not behave as guest molecules of clathrate compounds.

The temperature (T) dependence of the molar magnetic susceptibility (χ_M) of Mn^{II} complex (**1**) was measured from room temperature to 2 K (Fig. 3). Open circles show the experimental data plots. Curve fitting on Curie–Weiss law (solid line) gives a good agreement with the experimental data with Curie constant $C = 4.321$ emu K mol^{-1} and Weiss constant $\theta = -3.0$ K. The Curie constant obtained is consistent with the manganese high spin condition given by $S = 5/2$, $g = 1.99$. The Weiss constant $\theta = -3.0$ K shows that there is a weak antiferromagnetic interaction between magnetic moments on manganese cations through squarate anions.

$[M^{II}(C_4O_4)(C_4H_4N_2)(H_2O)_4]$ (M^{II} = Fe^{II} (2), Co^{II} (3), Ni^{II} (4), Cu^{II} (5), Zn^{II} (6)). X-ray single crystal structure determination performed on $[Zn^{II}(C_4O_4)(C_4H_4N_2)(H_2O)_4]$ complex revealed that the metal cation was coordinated by two pyrazine molecules and four water molecules in a distorted octahedral fashion. The pyrazine molecules bridge two metal centers through nitrogen atoms to make one-dimensional polymeric chain. Squarate anions exist among such one-dimensional chains to form four hydrogen bonds to water molecules coordinated to metal cations, forming a three-dimensional solid network as is shown in Fig. 4. The longest axis is the b axis.

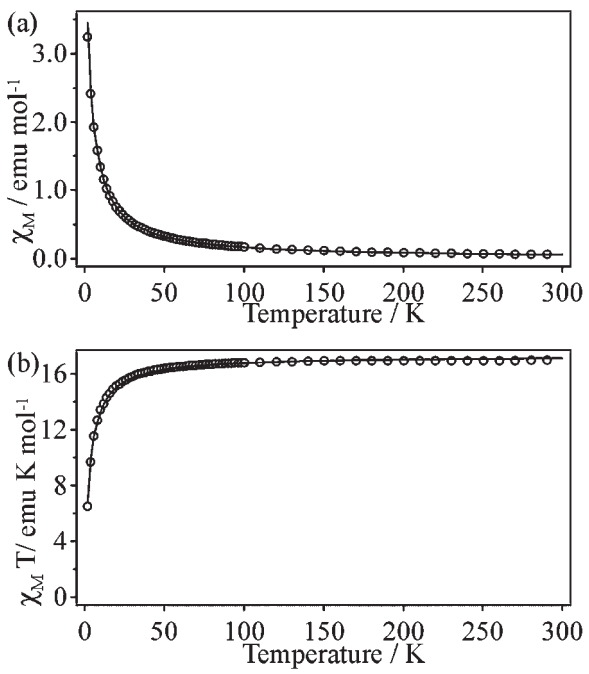

Fig. 3. Temperature dependence of χ_M (a) and $\chi_M T$ (b) for $[Mn^{II}_4(C_4O_4)_4(C_4H_4N_2)(H_2O)_8]$ (**1**). The solid line represents the best fit of the data (open circles) with the Curie–Weiss model.

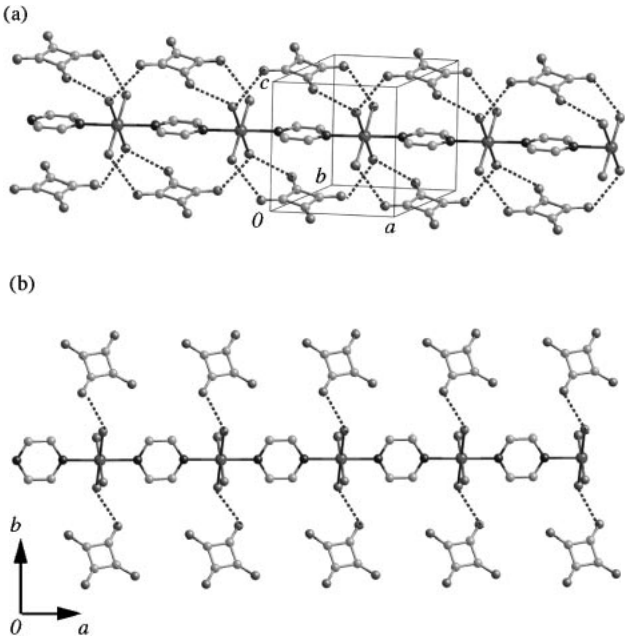

Fig. 4. (a) Three-dimensional network structure connected by hydrogen bonds between squarates and water molecules coordinated to Zn cations viewed from (a) the [010] direction and (b) the [001] direction. Dashed lines represent hydrogen bonds. Hydrogen atoms are omitted for clarity.

These results indicate that Zn^{II} complex (**6**) is isostructural with Ni^{II} complex (**4**) and Cu^{II} complex (**5**) as reported.[16,17]

The magnetic behaviors of these complexes were measured and the magnetic interactions were studied. The magnetic behaviors of Fe^{II} complex (**2**), Ni^{II} complex (**4**), and Cu^{II} complex (**5**) in the form of a $\chi_M T$ versus T plot [χ_M being the magnetic susceptibility per one metal(II) ion] are shown in Fig. 5(a). The extraporation of $\chi_M T$ values at the high temperature region for Fe^{II} complex (**2**), Ni^{II} complex (**4**), and Cu^{II} complex (**5**) suggested that they had typical values for quasi-isolated ions for $S = 2$, 1, and $1/2$ spin ground states, respectively. Calculated S values show that Fe^{II} complex (**2**) and Ni^{II} complex (**4**) are in high-spin state (Table 4). Upon cooling from room temperature, the $\chi_M T$ product decreased continuously down to 15 K and below 15 K more abruptly decreased down to 2.0 K. Thus small antiferromagnetic interactions exist between metal^{II} ions. The same character is shown by the χ_M–T curve for Cu^{II} complex (**5**) (Fig. 5(b) d). At room temperature, χ_M of Cu^{II} complex (**5**) was 0.00151 emu mol^{-1}. Upon cooling from room temperature, χ_M increased to a maximum value of 0.0323 emu mol^{-1} at 5.0 K. Below 5.0 K, there was a pronounced decrease down to 2 K ($\chi_M = 0.0278$ emu mol^{-1}). These anomalies at low temperature were similarly shown under the applied field parallel to the a, b and the c axis using a single crystal of Cu^{II} complex (**5**) (inserted figure of Fig. 5(b) e, f, g). These behaviors will be derived from an antiferromagnetic interaction which follows Bonner–Fischer's one-dimensional chain interaction as expected from the structural information. These magnetic data could be analyzed through the numerical expression for Bonner–Fischer's one-dimensional chain model for $S = 1/2$ as follows.[21]

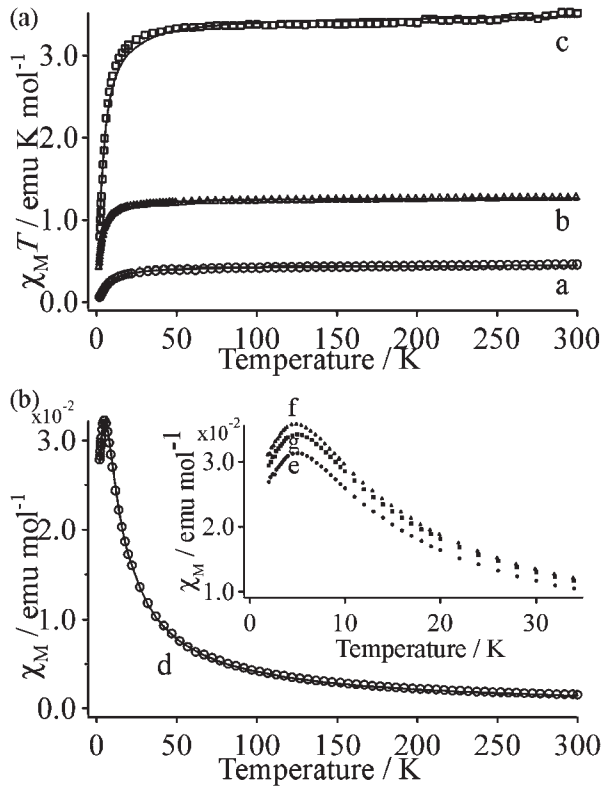

Fig. 5. (a) Temperature dependence of $\chi_M T$ for (a) Cu^{II} (**5**), (b) Ni^{II} (**4**), and (c) Fe^{II} (**2**) complexes using polycrystal samples. The solid line represents the best fit of the experimental data based on the Bonner–Fischer's one-dimensional chain model. (b) Temperature dependence of χ_M for Cu^{II} complex (**5**) using polycrystal samples (d). The solid line represents the best fit of the experimental data (open circles) with the Bonner–Fischer's one-dimensional chain model. Inserted figure shows temperature dependence of χ_M value of the single crystal of Cu^{II} complex (**5**) under the field of 0.5 T applied parallel to the *a*-axis (e), parallel to the *b*-axis (f), and parallel to the *c*-axis (g).

Table 4. Magnetic Parameters for Fe^{II} Complex (**2**), Ni^{II} Complex (**4**), and Cu^{II} Complex (**5**)

	2	**4**	**5**
S	2	1	1/2
g	2.29	2.27	2.18
J/k_B (K)	−0.9	−1.4	−7.8

$$\chi_M = Ng^2\beta^2(0.25 + 0.074975x + 0.075235x^2) / (1.0 + 0.9931x + 0.172135x^2 + 0.757825x^3)k_BT \quad (1a)$$
$$x = |J|/k_BT.$$

Symbols in this expression have their usual meanings. Least-squares fit (solid line) of the magnetic data leads to $g = 2.18$ and the antiferromagnetic exchange parameter $J/k_B = -7.8$ K for Cu^{II} complex (where J is the magnetic exchange coupling constant and k_B is the Boltzmann constant). The value estimated from the equation using the temperature which gives the maximum molar magnetic susceptibility ($kT_{max}/|J| = 0.641$) is −7.8 K, which is in good agreement with the value estimated from curve fitting.

In case of Ni^{II} complex (**4**), following numerical expression[22] was adopted.

$$\chi_M = Ng^2\beta^2(2.0 + 0.0194x + 0.0777x^2) / (3.0 + 4.346x + 3.232x^2 + 5.834x^3)k_BT \quad (1b)$$
$$x = |J|/k_BT.$$

The best fit was obtained in $g = 2.27$ and $J/k_B = -1.35$ K.

For Fe^{II} complex (**2**), an analytical expression for the magnetic susceptibility which treat the spins as classical spins,[21] is expected to be applicable:

$$\chi_M = (Ng^2\beta^2S(S+1)/3k_BT)(1+u)/(1-u) \quad (1c)$$
$$u = \coth(JS(S+1)/k_BT) - (k_BT/JS(S+1)).$$

The data are fitted by the theoretical curve with $g = 2.29$ and $J/k_B = -0.93$ K.

For Fe^{II} complex (**2**) and Ni^{II} complex (**4**), exchange parameters are smaller than those for Cu^{II} complex (**5**) as shown in Table 4. This difference is explained as follows. As to bond lengths between metals and ligands, M–N distance was smallest for Cu^{II} complex (**5**).[16,17] For Cu^{II} complex (**5**), elongation of the axial Cu–O bond (2.330 Å) due to Jahn–Teller distortion results in a compression of equatorial Cu–N bond (2.057 Å) and Cu–O bond (1.996 Å)[15] as usual.[23] This is considered to make metal to metal distance bridged by pyrazine molecule especially shorter, 6.887(1) Å, for Cu^{II} complex[17] than the others (7.247 Å for Fe^{II} complex (**2**), 7.042 Å for Ni^{II} complex (**4**), respectively).[16] This short distance is considered to strengthen the antiferromagnetic interaction in the chain direction.

In the case of Co^{II} complex (**3**), we measured the angular dependence of the magnetic susceptibilities on the single crystal and observed the clear anisotropy of the magnetic properties, as shown in Fig. 6. These differences along the three axes may be related to the zero-field splitting due to the crystal field around Co^{2+} with distorted-octahedral coordination of pyrazine and water molecules. When the ground state is split in zero-field into two Kramers doublets, the susceptibility parallel to the applied field is given by

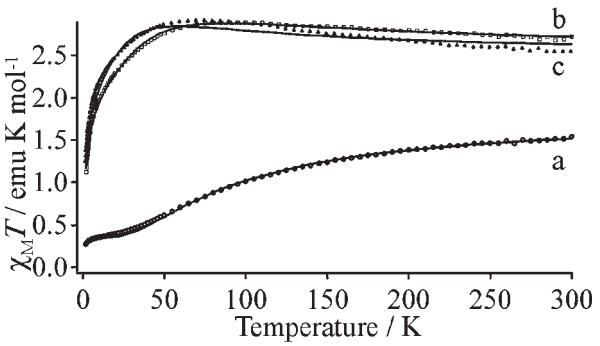

Fig. 6. Temperature dependence of $\chi_M T$ value of the single crystal of Co^{II} complex (**3**) measured under the field of 1 T parallel to the *a*-axis (a), parallel to the *b*-axis (b), and parallel to the *c*-axis (c). The solid line represents the best fit of the experimental data based on mean field theory.

$$\chi_a' = Ng_a{}^2\beta^2(1 + 9\exp(-2D/k_BT) /4kT(1 + \exp(-2D/k_BT)) \quad (2a)$$

and susceptibility perpendicular to the applied field is

$$\chi_{b,c}' = Ng_{b,c}{}^2\beta^2(1 + (3/4x[1 - \exp(-2x)]) /k_BT(1 + \exp(-2x)) \quad (2b)$$

with $x = D/k_BT$ using Van Vleck formula.[21] The macroscopic susceptibilities were corrected for the presence of exchange by means of a molecular-field approximation with zJ to afford equation

$$\chi_i = \chi_i'/(1 - (2zJ\chi_i'/Ng_i{}^2\mu_B{}^2)) \quad (2c)$$

i: a, b, c; z: nearest neighbor; J: exchange parameter. The fitting of the data using these equations (solid line in Fig. 6) resulted in $2D/k_B = 113$ K, $g_a = 1.97$, $g_b = 2.33$, $g_c = 2.31$, and $zJ/k_B = -1.6$ K. The difference of the g-values is considered to originate from the anisotropic nature of the g-tensor of the octahedral cobalt cation, and the small exchange parameter suggests the existence of a weak short-range antiferromagnetic interaction between the neighboring cobalt cations. The large value of the D parameter is in accordance with an octahedral Co^{II}, where the ground state doublet is well-isolated from the excited ones.

Conclusion

Squarate and pyrazine molecules react with the first-row transition metal cations in different fashions. The first type is Mn^{II} complex (**1**). Squarate dianion coordinates to Mn^{2+} to form a three dimensional network structure extended by hydrogen bonds. This network structure consisted of Mn^{2+} and squarate has cavities. Pyrazine molecules locate in these cavities through weak hydrogen bond interactions with the manganese(II) squarate network. Several studies have suggested that small molecules such as acetic acid hydrate or water molecules reside in the cavities as guest molecules. This time pyrazine molecules are found to locate stably in the cavities and their positions could be verified by crystal structure determination.

The second types are Fe^{II} (**2**), Co^{II} (**3**), Ni^{II} (**4**), Cu^{II} (**5**), and Zn^{II} (**6**) complexes. X-ray structure determination revealed that Zn^{II} complex (**6**) was isostructural to Ni^{II} (**4**) and Cu^{II} (**5**) complexes. Magnetic susceptibilities of Fe^{II} (**2**), Ni^{II} (**4**), and Cu^{II} (**5**) complexes are consistent with the Bonner–Fischer behavior, indicating the existence of the antiferromagnetic Heisenberg chain. The short metal to metal distance for Cu^{II} complex (**5**) gives larger antiferromagnetic exchange parameter than that of other complexes. In case of Co^{II} complex (**3**), the angular dependence of the magnetic susceptibility indicates that it has a large zero-field splitting and anisotropic g-tensor. The interaction between the nearest neighbor Co ions is weakly antiferromagnetic. Although Fe^{II} (**2**), Co^{II} (**3**), Ni^{II} (**4**), and Cu^{II} (**5**) complexes are almost isostructural, the difference of bond length and electronic state affect the magnetic interaction. These are considered to be important for the study of the magneto-structural correlations among quasi-one-dimensional structural complexes.

We studied the complex formation of divalent first-row transition metal anions from Mn^{2+} to Zn^{2+} in the aqueous solution containing squarate and pyrazine. Only Mn^{2+} was coordinated by squarate, and the rest were coordinated by pyrazine. One of the reasons for this difference can be explained by the concept of hard and soft acids and bases.

This work was funded by the Iwatani Naoji Foundation's Research Grant and also was supported by a Grant-in-aid for the 21st Century COE Program for Frontiers in Fundamental Chemistry from the Ministry of Education, Culture, Sports, Science and Technology. Prof. H. Kobayashi, Dr. E. Fujiwara, Dr. T. Otsuka, and Dr. H. Cui are gratefully acknowledged for helpful discussions and encouragement.

References

1 F. A. Cotton and C. Lin, *Acc. Chem. Res.*, **34**, 759 (2001).
2 Y. L. Cho, H. S. Uh, S. Y. Chang, N. G. Choi, I. J. Shin, and K. S. Jeong, *J. Am. Chem. Soc.*, **123**, 1258 (2001).
3 B. H. Hong, S. C. Bae, C. W. Lee, S. Jeong, and K. S. Kim, *Science*, **294**, 348 (2001).
4 G. J. Halder, C. J. Kepert, B. Moubaraki, K. S. Murray, and J. D. Cashoion, *Science*, **298**, 1762 (2002).
5 R. Kitaura, S. Kitagawa, Y. Kubota, T. C. Kobayashi, K. Kindo, Y. Mita, A. Matsuo, M. Kobayashi, H. C. Chang, T. C. Ozawa, M. Suzuki, M. Sakata, and M. Takata, *Science*, **298**, 2358 (2002).
6 M. Eddaoudi, J. Kim, N. Rosi, D. Vodak, J. Wachter, M. O'Keeffe, and O. M. Yaghi, *Science*, **295**, 469 (2002).
7 S. Cohen, J. R. Lacher, and J. D. Park, *J. Am. Chem. Soc.*, **81**, 3480 (1959).
8 R. West and D. L. Powell, *J. Am. Chem. Soc.*, **85**, 2577 (1963).
9 R. West and H. Y. Niu, *J. Am. Chem. Soc.*, **85**, 2589 (1963).
10 C. R. Lee, C. C. Wang, K. C. Chen, G. H. Lee, and Y. Wabg, *J. Phys. Chem.*, **103**, 156 (1999).
11 O. M. Yaghi, G. Li, and T. L. Groy, *J. Chem. Soc., Dalton Trans.*, **1995**, 727.
12 A. Weiss, E. Riegler, and C. Robl, *Z. Naturforsch.*, **41b**, 1333 (1986).
13 C. Naether, J. Greve, and I. Jess, *Acta Crystallogr.*, **E58**, m625 (2002).
14 O. Kahn, *Acc. Chem. Res.*, **33**, 647 (2000).
15 J. A. Real, G. De Munno, M. C. Munoz, and M. Julve, *Inorg. Chem.*, **30**, 2701 (1991).
16 C. Naether, J. Greve, and I. Jess, *Z. Naturforsch.*, **58b**, 52 (2003).
17 O. M. Yaghi, G. Li, and T. L. Groy, *J. Solid State Chem.*, **117**, 256 (1995).
18 T. Steiner and G. R. Desiraju, *Chem. Commun.*, **1998**, 891.
19 G. With, S. Harkema, and D. Feil, *Acta Crystallogr.*, **B32**, 3178 (1976).
20 V. R. Thalladi, A. Gehrke, and R. Bese, *New J. Chem.*, **24**, 463 (2000).
21 O. Kahn, "In Molecular Magnetism," VCH, New York (1993), and references therein.
22 A. Meyer, A. Gleizes, J. J. Girerd, M. Verdaguer, and O. Kahn, *Inorg. Chem.*, **21**, 1729 (1982).
23 G. J. Grant, M. W. Jones, K. D. Loveday, D. D. VanDerveer, W. T. Pennington, C. T. Dagle, and L. F. Mehne, *Inorg. Chim. Acta*, **300–302**, 250 (2000).